Optimization of planform and cruise conditions of a transport flying wing

R Martinez-Val*, E Perez, J Puertas, and **J Roa**
Universidad Politecnica de Madrid, Madrid, Spain

Abstract: The flying wing is a promising concept for the mid long-term commercial aviation. After the previously published conceptual design of a 300-seat class flying wing, the present article carries out a parametric analysis to optimize its planform and analyse the suitable cruise conditions to achieve the highest efficiency of such configuration. The figures of merit chosen for the optimization are the direct operating cost and the maximum take-off weight per passenger, for a specified constant range of 10 000 km. The design has to respect five relevant constraints: wingspan (limited to 80 m), cabin width, wing tip chord, number of passengers, and cruise lift coefficient. The optimum aircraft fulfilling all constraints cruises at 45 000–47 000 ft and $M = 0.82$, has an aspect ratio of 6.3 and taper ratio of 0.10, and carries about 280 passengers in three-class seating. This aircraft is about 20 per cent more efficient than conventional wide bodies of similar size, in terms of trip fuel.

Keywords: flying wing, optimization, conceptual design

1 INTRODUCTION

Commercial aviation of the jet era has been based on what is currently called the conventional layout. This is characterized by a slender fuselage mated to a high aspect ratio wing, with horizontal and vertical tailplanes fitted to the fuselage tail cone, and pod-mounted engines under the wing [**1**]. A variant, with engines attached to the rear fuselage, was also developed during the 1950s and is still broadly used in business and regional jets. The conventional arrangement has been incorporating all improvements in aerodynamics, propulsion, materials, avionics, etc., over the years. As a consequence, the airliners are now about 100 per cent more efficient than 50 years ago, in terms of range parameter [**2**]. However, it seems that this configuration is approaching an asymptote around the size of A380 in its productivity and capacity characteristics [**3**, **4**], and this is happening in a period of increasing environmental concern about pollution and noise [**5–7**].

What designs will be better matched to the aforementioned scenario within two or three decades? One of the configurations under study is the flying wing in its different concepts: blended-wing body, C-wing, U-wing, tail-less aircraft, etc. [**8–17**]. The introduction of a new paradigm must be backed up by suitable analysis, albeit of an approximate nature, of relevant issues such as productivity, airport compatibility, passenger acceptance, etc. In the case of flying wings, open literature indicates that this layout may provide significant fuel savings and, hence, a lower level of pollution compared to conventional designs. Moreover, according to the published research, the engine intakes would be above the wing and the aircraft would require none or very limited high-lift devices in low-speed operations, which would result in a quiet airplane. These findings explain the great deal of activity carried out by the aircraft industry and numerous researchers to perform conceptual design studies and identify problems and challenges posed by this layout. Most articles deal with very-high-capacity aircraft, up to 1000 passengers, but the forecasts are very promising for medium-capacity flying wings too.

The conceptual design of a 300-seat class flying wing, including technical feasibility and operational efficiency aspects, has been described in some former articles [**18–22**]. Not only is the flying wing 15–20

per cent more efficient in cruise but it also requires shorter take-off and landing distances and generates a less intense vortex wake, thus increasing airport and airways capacities. The present article concentrates on optimizing the cruise Mach number and wing planform, namely the aspect and taper ratios, of such concept by means of a parametric analysis. The process is carried out subject to five operational and design constraints, which will duly be described later: the new International Civil Aviation Organisation (ICAO) 80 m wingspan limit, cabin width, wing tip chord, number of passengers and cruise lift coefficient. The range is kept constant during the process at 10 000 km and the cruise mid-point altitude is assumed to be 45 000 ft, from a former first approximation analysis. Once the flying wing planform is optimized, the specific range (range per unit mass of fuel burnt) is obtained for several flying altitudes, in order to confirm the suitability of the 45 000 ft hypothesis and the penalties associated with non-optimum conditions.

2 THE C-FLYING WING CONFIGURATION

The main features of the C-type flying wing used in the present research are described in detail in reference [**20**]. Its initial specifications correspond to a common long-range mission: 10 000 km with a full passenger load (around 250–300 passengers) at high subsonic speed (Mach number between 0.8 and 0.85). This mission covers most relevant routes between Europe and USA, West US coast to Far East, etc. [**5**, **6**].

Except for a nose bullet in the apex to accommodate the cockpit with adequate visibility, the leading and trailing edges are perfectly straight. Figure 1 depicts the overall external as well as internal arrangement of the aircraft. The wing spars are located at 11 per cent and 67 per cent of the chord. These values provide a suitable balance between structural strength and rigidity on one side and habitability on the other side [**20**]. Table 1 depicts the key variables of the C-layout conceptual design.

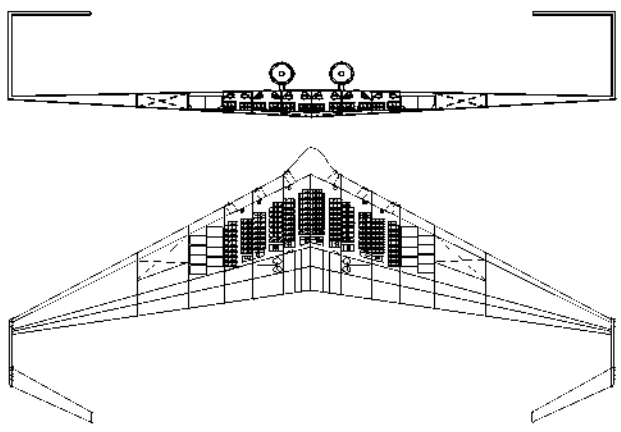

Fig. 1 Two-view sketch of the C flying wing

Table 1 Main features of a non-optimized flying wing conceptual design

Variable	Value
Overall length (m)	46
Overall width (m)	77
Height above ground (m)	16
Wing area (m^2)	893
Wingspan (m)	75
Aspect ratio	6.3
Taper ratio	0.11
$c/4$ swept angle (degree)	30
Cabin area (m^2)	230
Three-class capacity	240
MTOW (kg)	205 000
OEW (kg)	109 000
MPL (kg)	35 000
MFW (kg)	75 000
Thrust-to-weight ratio at take-off	0.25
Maximum wing loading (Pa)	2250

The C-wing layout exhibits the minimum induced drag among various alternatives [**9**]. As indicated in the Introduction, the 80 m wingspan limit of ICAO F category [**23**] has been respected. To allow outer bending of the wing-tip-attached empennages, the actual wingspan is limited to 77 m. This limitation has a deep influence on the design, as it will be shown below.

In a payload-driven design, such as the flying wing [**12**, **16**], the cabin area is a variable of maximum relevance. This area can be expressed as

$$\frac{S_{\text{cab}}}{S} = f\left(A, \lambda, \frac{t}{c}, \text{inner arrangement, etc.}\right) \tag{1}$$

where S_{cab} stands for cabin area, S wing gross area, A aspect ratio, λ taper ratio, and t/c relative thickness.

By definition, wing gross area, wingspan (b), and aspect ratio are linked through $A = b^2/S$.

On the other hand, in a pure flying wing the wetted area (the dominant term in aerodynamic drag) is related to the internal volume and the airfoil relative thickness (assumed constant spanwise) as

$$\frac{\text{Wetted area}}{(\text{Volume})^{2/3}} \propto A^{1/3}\left(\frac{t}{c}\right)^{-2/3} \tag{2}$$

Therefore, to obtain the best from its inherent characteristics the flying wing must be designed with a higher relative thickness and lower aspect ratio than its conventional counterparts. Slightly aft loaded, 17 per cent thick airfoils are used in the outer part of the wing, whereas upward rear curvature airfoils with similar thickness are employed in the central part for trimming purposes [**14**, **24**]. Such uncommon thickness is just in the admissible region according to reference [**25**]

$$\frac{t}{c} \leqslant (0.95 - 0.1C_{\text{Lcr}}) - (M_{\text{nom}} + 0.02)\cos^{0.5}\Lambda \tag{3}$$

where C_{Lcr} and M_{nom} stand for cruise lift coefficient and design Mach number, respectively, and Λ is the quarter chord swept angle.

Structurally, the flying wing is arranged as a dual entity: an unconventional inner wing with a pressurized torque box between the spars, for passenger cabins and holds, and an outer wing with fairly conventional architecture, including fuel tanks outboard of the cargo holds. The inner wing is arranged as a vaulted double-skin, ribbed shell that behaves very well in terms of weight saving, load diffusion, and fail-safe features [**11**, **19**, **20**].

Figure 2 shows the internal cabin arrangement in a three-class seating for about 250 passengers. Exit doors are provided as follows: two symmetric pairs through the leading edge of the aircraft plus one symmetric pair at the rear; all of them type A size. Cabin cleaning and servicing can be performed without interfering with passengers, by using the rear doors, thus shortening the turnaround time of the aircraft.

It is important to notice that this aircraft must fly higher than conventional airliners for its different drag polar parameters and low wing loading. In effect, for a common parabolic drag polar, i.e. $C_D = C_{D0} + C_L^2/(\pi A\varphi)$ and a current technology turbofan, with specific fuel consumption varying as $c_j \sim M^\beta\sqrt{\theta}$ [**26**, **27**], the lift coefficient for an efficient cruise is

$$C_{Lcr} = \sqrt{\beta C_{D0}\pi A\varphi} \tag{4}$$

where β is a parameter related to the Mach number dependence of the specific fuel consumption (see equation (12)), about 0.5 for current high bypass ratio turbofans; C_{D0} is the constant term in the drag polar;

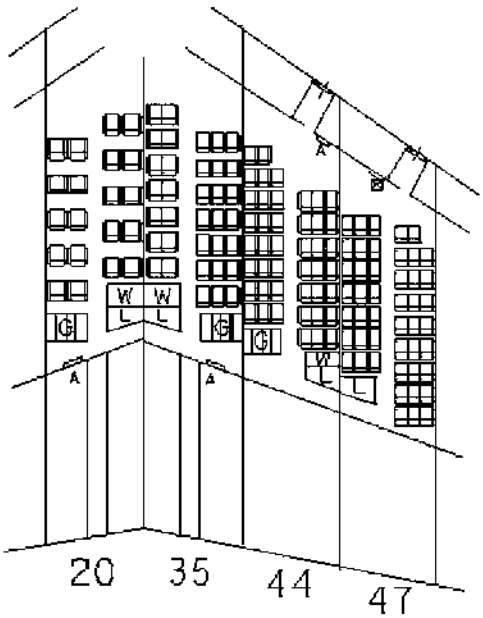

Fig. 2 Potential three-class seating arrangement for 250 passengers. The outer bays are symmetrical

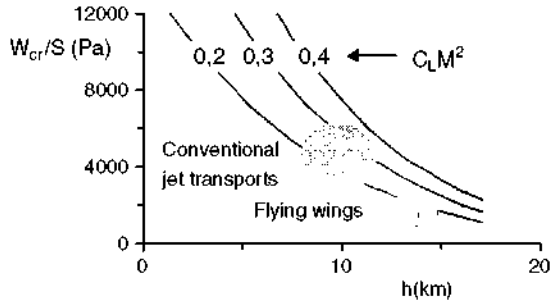

Fig. 3 Cruise conditions for conventional transport airplanes and flying wings [**20**]

and φ is the induced drag efficiency factor (between 0.75 and 0.9 in most cases) [**25**, **28**].

From the vertical balance of forces, lift equals weight; i.e. $W_{cr} = L = (\gamma/2)pM^2SC_{Lcr}$. Therefore, from equation (4) the pressure altitude in cruise is

$$p = \frac{2W_{cr}/S}{\gamma M^2\sqrt{\beta C_{D0}\pi A\varphi}} \tag{5}$$

where γ is 1.4 and p, M, and W_{cr} are pressure, Mach number, and weight in cruise conditions, respectively. As indicated in Fig. 3 (from reference [**20**]), the flying wings have to fly higher than conventional airliners to obtain the maximum benefits from its aerodynamic and propulsive characteristics.

The centre of gravity of the empty flying wing is at 32 per cent of the mean aerodynamic chord, and most conditions fall within a 28–34 per cent range, much shorter than in common transport aircraft [**28**, **29**]. These values are in perfect agreement with the location of the aerodynamic centre, which is estimated to be at 32 per cent in cruise, and slightly ahead in low-speed conditions.

As shown in reference [**20**], this C-type flying wing requires about 15 per cent less trip fuel than similar-capacity aircraft, such as A330-200 and B777-200, and it is capable of taking off and landing in only 1800 and 1300 m, respectively.

3 OPTIMIZATION PROCESS

Optimizing the wing planform means finding the values for the aspect ratio A, taper ratio λ, and swept angle Λ, which provide an optimum for certain figure of merit. The quarter chord swept angle, Λ, is directly linked to the design Mach number, relative thickness (17 per cent), and cruise lift coefficient (~0.20) through equation (3).

Two different figures of merit are used in the present study to increase the robustness of the whole procedure: the direct operating cost (DOC) and the maximum take-off weight per passenger W_{to}/N_{pax}, in the understanding that both variables are representative of efficient performance and good design [**25**, **28**].

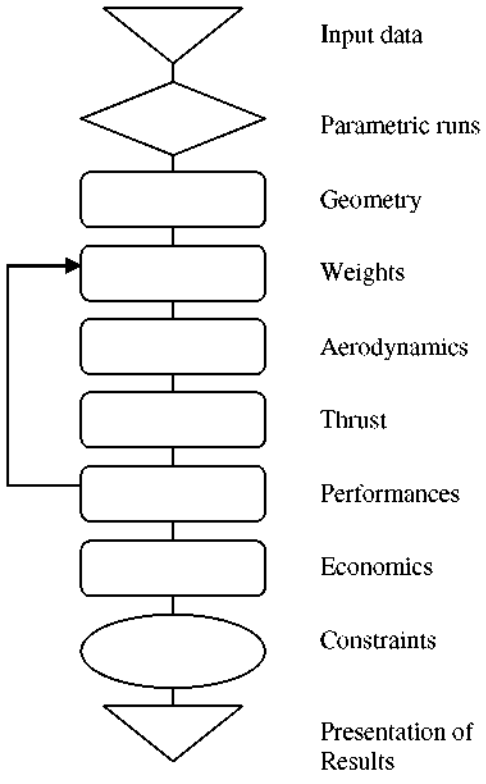

Fig. 4 Process chain used for optimization

The process chain is presented in Fig. 4. It includes six modules devoted to wing and cabin geometries, aircraft main weights, aerodynamics, thrust, performances, and economics. As trip fuel, maximum take-off weight, etc. depend on the performances and, on its turn, the performances depend on the aircraft weight, the process incorporates an iteration loop. At the end of the chain, the results are confronted with the following operational and design constraints:

(a) cabin half-width, smaller than 7.9 m, equivalent to two generous narrow body bays, for emergency evacuation considerations and to avoid large vertical acceleration in bank manoeuvres;
(b) wing tip chord, larger than 2.2 m, for structural reasons, because half T empennages are fitted to each tip (see Fig. 1);
(c) number of passengers, below 315 to give a margin with respect to the maximum acceptable of 330, for emergency evacuation reasons;
(d) cruise lift coefficient, smaller than 0.275, to assure acceptable cabin attitudes in flight and to avoid buffet onset in manoeuvres, in this thick airfoil.

Following the process chain of Fig. 4, the geometry module starts by computing S, S_{cab}, and the aircraft capacity N_{pax}, in three-class seating

$$S = \frac{b^2}{A} \tag{6}$$

$$S_{\text{cab}} = 0.14A\left(\frac{1+\lambda}{1-\lambda}\right)\left[\frac{4b^2}{A^2(1+\lambda)^2} - c_{\text{min}}^2\right] \tag{7}$$

$$N_{\text{pax}} = 0.96 S_{\text{cab}} \tag{8}$$

where S_{cab} is the cabin area in square metres. The parameter c_{min} (equal to 15 m) appearing in equation (7) is imposed by airfoil geometry and spar location for habitability.

On the other side, equation (8) represents about 10 per cent extra room per passenger with respect to conventional transport airplanes in the category [**30**, **31**] to account for slanted corridors, thick ribs for bay separation, etc.

In the mass module, the main weights are related as follows

$$\text{MTOW} = \text{OEW} + \text{PL} + \text{TF} + \text{RF} \tag{9}$$

where MTOW indicates maximum take-off weight, OEW operating empty weight, PL payload, TF trip fuel, and RF reserve fuel. On its turn, the operating empty weight is decomposed among structure, equipment, furniture, crew, and other operational items. Their contributions are computed in terms of MTOW, S_{cab}, and N_{pax} following the common conceptual design-level expressions [**28**, **29**, **32**]. The reserve fuel is estimated to be 5 per cent of the landing weight [**25**, **28**, **32**]. Payload is estimated as 100 kg per passenger, plus extra cargo in the available space of the freighthold. Finally, the trip fuel is computed as

$$\text{TF} = 0.05\,\text{MTOW} + 0.97\,\text{MTOW}[1 - \text{e}^{-(9700/K)}] \tag{10}$$

The first right-hand term represents the fuel consumption in the non-cruise phases of the trip [**32**, **33**]. The 0.97 factor indicates the weight fraction at the cruise start with respect to MTOW, at a high flight level [**33**]. On the other side, the design range, i.e. 10 000 km, has been shortened by 300 km to compensate for the distance flown in climbing and descent.

The average range parameter, K, depends on the cruise speed, V, specific fuel consumption, c_j, and lift over drag ratio, L/D, as

$$K = \frac{V}{c_j}\frac{L}{D} \tag{11}$$

which, with $c_j = 0.62\,M^{\beta}\sqrt{\theta}$ [**26**, **27**] and some mathematical manipulation, yields

$$K = \frac{M_{\text{nom}} a_{\text{tp}}}{0.62\,M_{\text{nom}}^{0.5}}\frac{C_{\text{L}}}{C_{\text{D}}} \tag{12}$$

where a_{tp} is the speed of sound at or above the tropopause, and the aerodynamic ratio has been substituted by the coefficients ratio. The Mach number dependence of the specific fuel consumption [**26**, **27**]

is explicitly shown in the first denominator. Therefore, the range parameter can be expressed as

$$K = 1713\, M_{\text{nom}}^{0.5} \frac{C_{\text{L}}}{C_{\text{D}}} \tag{13}$$

where the factor 1713 is in kilometres. By assuming that the typical mid-cruise takes place at 45 000 ft [20], the lift coefficient is

$$C_{\text{L}} = 9.50 \times 10^{-4} \frac{\text{MTOW} - \text{TF}/2}{M_{\text{nom}}^2 S} \tag{14}$$

where MTOW and TF are expressed in kilograms and S in square metres. For the present study, the drag polar is represented by a common parabolic relationship

$$C_{\text{D}} = C_{\text{D0}} + \frac{C_{\text{L}}^2}{0.9\pi A} \tag{15}$$

The 0.9 factor in the denominator of the lift-dependent part includes the effect of the vertical stabilizers to diminish the vortex wake [9]. The first right-hand term is estimated as follows [34]

$$C_{\text{D0}} = 3.96 c_{\text{f}} \left[1 + \frac{0.085}{(1+\lambda)}\right] \cos^{0.15} \Lambda + 3.578 \left[M_{\text{nom}} - \frac{0.71}{\cos^{0.5} \Lambda}\right]^{2.5} \tag{16}$$

As the swept angle is matched to the design Mach number, the wave drag contribution is only about 0.001 for all cases considered. Although the flying wing concept is very appropriate for incorporating laminar flow control and other emerging technologies [20], the present study considers that only the first 15 per cent of the chord has a laminar boundary layer. The friction coefficient is, thus, estimated as

$$c_{\text{f}} = 0.198 Re^{-0.5} + 0.365 (\log Re)^{-2.58} \tag{17}$$

As shown in Fig. 4, DOC is estimated at the end of the process. DOC is not estimated here in absolute terms (which is beyond the scope of the present research and would have many unknown input data), but in relative terms with respect to a baseline design established in a previous analysis [20], which carries 280 passengers at $M_{\text{nom}} = 0.80$, with MTOW (W_{toref}) equal to 215 000 kg and reference trip fuel TF_{ref} of 59 000 kg. As usual, DOC includes the contributions related to aircraft price, crew, fuel, airport and navigation taxes, and maintenance. Explicitly this means

$$\text{DOC} = C_{\text{price}} + C_{\text{crew}} + C_{\text{fuel}} + C_{\text{tax}} + C_{\text{maint}} \tag{18}$$

Because of being a relative DOC, it is equal to 1.00 for the arbitrary baseline data. A typical sharing for a medium-size wide body in a long-range mission is 25 per cent, 12 per cent, 33 per cent, 15 per cent, and 15 per cent, respectively [35, 36], and this sharing has been taken in the present computations for the baseline design. The contributions are assumed to vary with MTOW, the flying block time (cruise time plus half an hour, i.e. $0.5 + 9.42/M_{\text{nom}}$), and the number of passengers [35–37]. Various contributions are computed as

$$C_{\text{price}} = 0.25 \frac{W_{\text{to}}}{W_{\text{toref}}} \left(\frac{9.42}{M_{\text{nom}}} + 0.5\right) \frac{23}{N_{\text{pax}}} \tag{19}$$

$$C_{\text{crew}} = \left(0.07 + \frac{0.05\, N_{\text{pax}}}{280}\right) \left(\frac{9.42}{M_{\text{nom}}} + 1\right) \frac{22.1}{N_{\text{pax}}} \tag{20}$$

$$C_{\text{fuel}} = 0.33 \frac{\text{TF}}{\text{TF}_{\text{ref}}} \frac{280}{N_{\text{pax}}} \tag{21}$$

$$C_{\text{tax}} = \left[0.07 \left(\frac{W_{\text{to}}}{W_{\text{toref}}}\right)^{0.7} + 0.08 \frac{N_{\text{pax}}}{280}\right] \frac{280}{N_{\text{pax}}} \tag{22}$$

$$C_{\text{maint}} = 0.15 \left(\frac{W_{\text{to}}}{W_{\text{toref}}}\right)^{0.7} \left(\frac{9.42}{M_{\text{nom}}} + 0.5\right) \frac{23}{N_{\text{pax}}} \tag{23}$$

As it is usual in DOC studies, the crew block time in equation (20) is considered half an hour longer ($1 + 9.42/M_{\text{nom}}$) than the flying block time [35–37].

4 PARAMETRIC RESULTS

The whole process is repeated for $M_{\text{nom}} = 0.8$, 0.82, and 0.85, and, according to previous analysis, the aspect ratio is studied within the 5.6–7 range and the taper ratio between 0.08 and 0.28.

All results are gathered in spread sheets and plots, for the diverse M_{nom}, A, and λ combinations. Four columns are added with flag codes to indicate whether the aforementioned constraints are surpassed. The airfoil characteristics, wing spar location (11 per cent and 67 per cent of chord), wingspan ($b = 77$ m), and range ($R = 10\,000$ km) are assumed to be constant during the process, corresponding to the values defined in the conceptual design [20].

For each design case, i.e. the constant initial input data (range, structural arrangement, airfoil relative thickness, etc.), plus a given set of A, λ, and M_{nom}, the procedure provides values for a large number of variables: wing area, cabin surface, swept angle, number of passengers, maximum take-off weight, operating empty weight, payload, trip and reserve fuel, mid-cruise lift over drag ratio, and DOC. It must be recalled that DOC is estimated only in relative terms, with respect to an initial reference. The second figure of merit, i.e. the maximum take-off weight per passenger, is then easily computed from the former variables.

Figures 5 and 6 show DOC and $W_{\text{to}}/N_{\text{pax}}$ as a function of aspect ratio and taper ratio for $M_{\text{nom}} = 0.8$; the acceptable results, respecting all constraints, are shown in thick lines. The plots also depict, to the bottom-left corner, the boundaries corresponding to

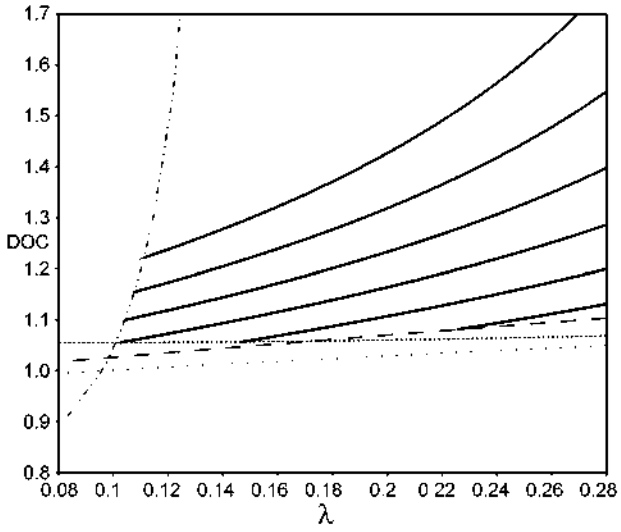

Fig. 5 Constrained results of relative DOC in terms of aspect ratio and taper ratio for $M_{nom} = 0.8$. From top to bottom $A = 7$, 6.8, 6.6, 6.4, 6.2, and 6. The boundaries of acceptable values correspond to the following design constraints: ---●●--- is for $c_t \geqslant 2.2$ m, --- for $y_{cmin} \leqslant 7.9$ m, ··· for $C_L \leqslant 0.275$, and ··· for N_{paxmax}

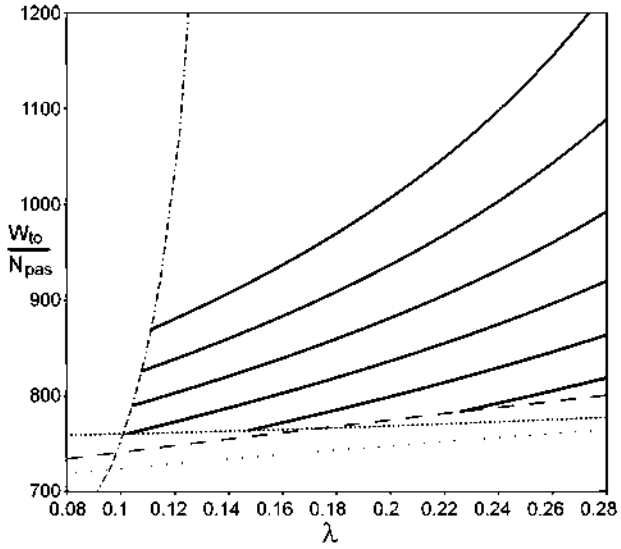

Fig. 6 Same as Fig. 5 but for maximum take-off weight per passenger

various design constraints considered in the present analysis: tip chord, c_t; spanwise location of minimum airfoil chord, y_{cmin}; and cruise lift coefficient, C_L. The limitation in the number of passengers never affects the results. The mathematical minimum (with zero first derivatives) falls beyond the envelope of A and λ values studied, for it is not realistic and does not respect the design constraints. The constrained optimum for DOC corresponds to $A = 6.41$ and $\lambda = 0.101$, which are values quite apart from those of conventional airliners, typically in the 7–10 and 0.2–0.25 ranges, respectively. The DOC minimum is very flat, with several A–λ combinations that provide DOC values close to the optimum. As a matter of fact, between the A–λ points 6.1–0.18 and 6.4–0.1, the DOC hardly varies by 2 per cent. This result is very interesting because it provides some degree of freedom for the designers, who could thus trade other design or operational constraints.

At higher M_{nom}, i.e. 0.82 and 0.85, the A and λ values for an optimum DOC change very little: in both cases they are $A = 6.3$ and $\lambda = 0.10$. The absolute DOC minimum, within the accepted A–λ–M_{nom} space occurs at $M_{nom} = 0.85$ and it is just 1.7 per cent smaller than the one at 0.8.

The former arguments and comments apply with respect to W_{to}/N_{pax}, although the absolute minimum in this figure of merit corresponds to $M_{nom} = 0.82$, with $A = 6.3$ and $\lambda = 0.10$ as well. Such optimum corresponds not only to 760 kg/pax, well below the values of A330-200 (890 kg/pax) and B777-200 (920 kg/pax), but also below those of B747-400 (860 kg/pax) or A380-800 (920 kg/pax).

As indicated earlier, because the mathematical optimum falls beyond the envelope of acceptable A and λ values, the optimum does not imply a first zero derivative of DOC or W_{to}/N_{pax} with respect to such variables. On the other hand, it must be realized that the results are more dependent on the aspect ratio than on the taper ratio. This is clearly observed in Figs 5 and 6 and can be quantified by computing the non-dimensional sensitivity derivatives near the constrained optimum. For example, for $M_{nom} = 0.8$ the corresponding values are

$$\frac{\partial \mathrm{DOC}}{\partial A}\frac{A}{\mathrm{DOC}} = 1.26 \quad \text{and} \quad \frac{\partial \mathrm{DOC}}{\partial \lambda}\frac{\lambda}{\mathrm{DOC}} = 0.13 \tag{24}$$

for the DOC, and

$$\frac{\partial \mathrm{Wn}}{\partial A}\frac{A}{\mathrm{Wn}} = 1.15 \quad \text{and} \quad \frac{\partial \mathrm{Wn}}{\partial \lambda}\frac{\lambda}{\mathrm{Wn}} = 0.13 \tag{25}$$

for the maximum take-off weight per passenger. For clarity, the variable W_{to}/N_{pax} has been substituted by Wn in equation (25).

5 OPTIMUM CRUISE CONDITIONS

The former section has been devoted to establish the best wing planform for the aircraft, within the design space allowed by the constraints. Now, once the geometry, aerodynamics, and other related variables are known, the next step is to confirm that the 45 000 ft level chosen as the flying altitude is the most appropriate one for mid-cruise of such a long trip. Needless to say that the flight will require various cruise altitudes, typically three constant level segments [**28**, **32**, **35**], that should match the decreasing weight.

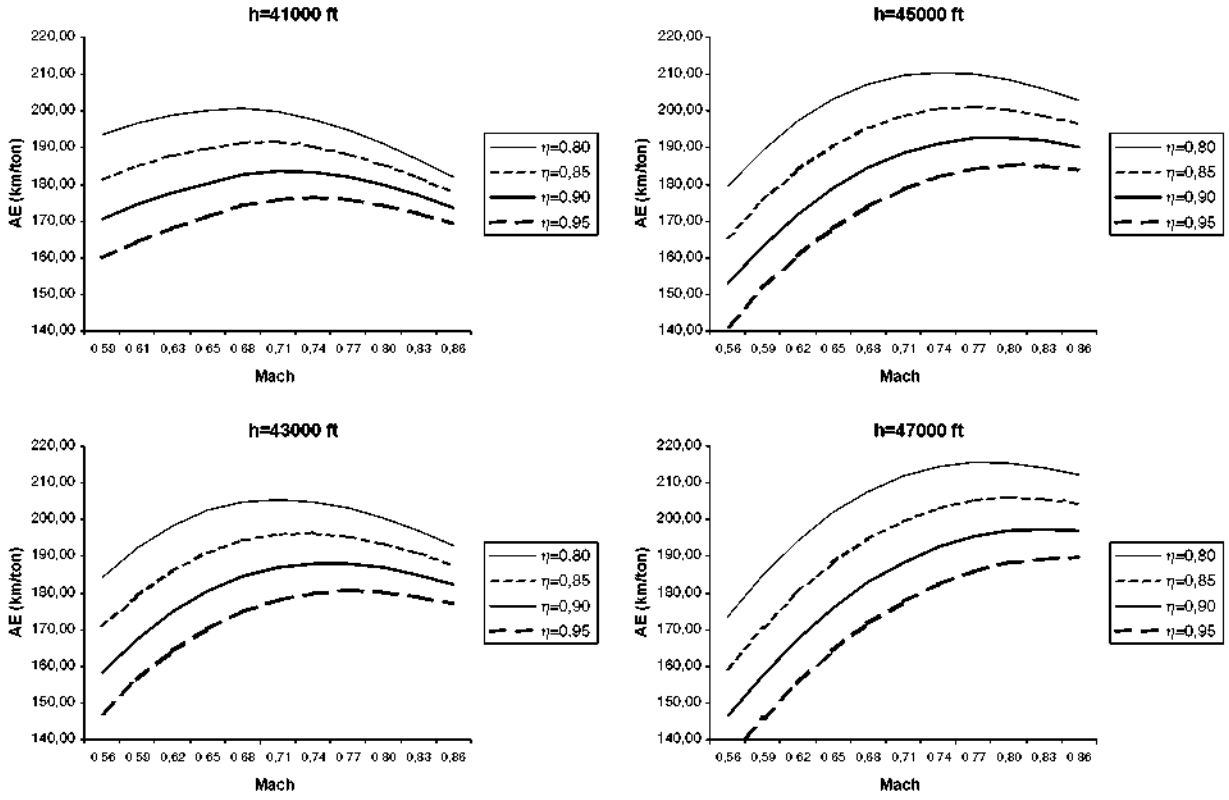

Fig. 7 Specific range, AE, for $M_{\text{nom}} = 0.82$ in terms of cruise Mach number and weight fraction ($\eta = W_{\text{cr}}/\text{MTOW}$) for various cruise altitudes

The specific range is the key variable for this purpose. Following the definition of specific fuel consumption, the range travelled per unit of fuel mass burnt becomes

$$\frac{\mathrm{d}R}{\mathrm{d}W} = -\frac{Ma_{\text{tp}}}{c_j}\frac{L}{D}\frac{1}{W} \tag{26}$$

Figure 7 presents the specific range for a flying wing optimized for $M_{\text{nom}} = 0.82$. Although the aircraft has been designed for such speed, it will actually fly at varying levels and Mach numbers. Thus, Fig. 7 shows the distance flown per unit of fuel mass burnt, AE, as a function of M at various flight levels, for four weight fractions, namely $W_{\text{cr}}/\text{MTOW} = 0.80$, 0.85, 0.90, and 0.95. The x-axis is always limited to $M = 0.86$ and, consequently, the figure does not depict the sharp decline produced by the drag rise on the right-hand side.

The results indicate that the aircraft gains efficiency at very high flight levels, about 45 000–47 000 ft. On the other side, as expected, the optimum Mach number increases with the aircraft weight, always being slightly smaller (one- or two-hundredths) than the design Mach number, because the overall optimization process includes economics and other factors.

For $M_{\text{nom}} = 0.82$ the initial optimum cruise (at about 0.95 MTOW) would be at $M_{\text{cr}} = 0.81$ and 45 000 ft, with a specific range of 0.185 km/kg. Later in the flight, when the weight has been reduced to 0.90 MTOW, the optimum cruise can be either at $M_{\text{cr}} = 0.81$ and 45 000 ft or at $M_{\text{cr}} = 0.82$ and 47 000 ft, in both cases with a specific range of about 0.195 km/kg. Finally, when the flight is near the end and the aircraft weight is about 0.80 MTOW, the flying wing should cruise at $M_{\text{cr}} = 0.81$ and 47 000 ft to reach an astounding 0.215 km/kg. This last value is equivalent to 2.04 l per pax per 100 km, or 57 g CO_2 per passenger.kilometre, which are very good marks even for compact cars, but at about 870 km/h instead of about 100 km/h [22].

The aircraft designed for $M_{\text{nom}} = 0.80$ or 0.85 is almost as good as the former one, with optimum specific ranges just 2–3 per cent below the aforementioned values. The only difference is that at $M_{\text{nom}} = 0.80$ the optimum cruise remains longer at 45 000 ft, and for $M_{\text{nom}} = 0.85$ the cruise should always take place at 47 000 ft.

6 CONCLUSIONS

The flying wing is a promising configuration for future transport aircraft. Previously published details of conceptual designs show that such an aircraft would require about 15–20 per cent less fuel than its conventional counterparts, need shorter runways for airport operations, and produce a less intense wake,

which would result in a remarkable increase in the airport capacity. Not only very large aircraft, in the 800–1000-seat class, could be feasible and efficient, the medium-size category could also beat conventional airliners in the 300-seat class.

The specific conclusions of the present research are as follows.

1. According to the sensitivity analysis carried out, the aspect ratio is more important for optimizing the wing planform than the taper ratio, although both are linked to structural constraints that impede reaching the absolute optimum.
2. The optimum flying wing, fulfilling a series of relevant design and operational constraints, has a planform defined by an aspect ratio of 6.3 and a taper ratio of 0.10, values that fall quite apart from those found in common transport jets.
3. The constrained optimum corresponds to a flying wing that carries about 280 passengers at 760 kg of maximum take-off weight per passenger, for a 10 000 km route.
4. To fully benefit from its inherent characteristics, a transport flying wing must cruise at about $M_{cr} = 0.82$ and 45 000–47 000 ft, thus freeing lower, more congested airways.

In the last tier of its trip, a medium-size flying wing would be as efficient as a compact car, in terms of fuel burnt (2.1 l per passenger per 100 km) or CO_2 produced (57 g per passenger.kilometre), but at 870 instead of 100 km/h.

REFERENCES

1 **Anderson, J. D.** *The airplane: a history of its technology*, 2002 (AIAA, Reston, Virginia).
2 **Martinez-Val, R., Palacin, J. E.,** and **Perez, E.** The evolution of jet airliners explained through the range equation. *Proc. IMechE, Part G: J. Aerospace Engineering*, 2008, **222**, 915–919. DOI: 10.1243/09544100JAERO338.
3 **Martinez-Val, R., Perez, E., Muñoz, T.,** and **Cuerno, C.** Design constraints in the payload-range diagram of ultrahigh capacity transport airplanes. *J. Aircraft*, 1994, **31**, 1268–1272.
4 **Champion, C.** The A380 programme. In Proceedings of the 26th ICAS Congress, Anchorage, Alaska, USA, September 2008 (available on CD-ROM).
5 Global Market Forecast. 2007–2026, Airbus, Blagnac (*F*), 2007.
6 Current Market Outlook. 2008–2027, Boeing Commercial Airplanes, Seattle, Washington, 2008.
7 **Martinez-Val, R.** and **Perez, E.** Aeronautics and astronautics: recent progress and future trends. *Proc. IMechE, Part C: J. Mechanical Engineering Science*, 2009, **223**, 2767–2820. DOI: 10.1243/09544062JMES1546.
8 **Nickel, K.** and **Wohlfahrt, M.** *Tailless aircraft: in theory and practice*, 1994 (Arnold, London, UK).
9 **McMasters, J. H.** and **Kroo, I. M.** Advanced configurations for very large transport airplanes. *Aircraft Design*, 1998, **1**, 217–242.
10 **Bolsunovski, A. L., Buzoverya, N. P., Gurevich, B. I., Denisov, V. E., Dunaevski, A. I., Shkadov, L. M., Sonin, O. V., Udzhukhu, A. J.,** and **Zhurihin, J. P.** Flying wing – problems and decisions. *Aircraft Design*, 2001, **4**, 193–219.
11 **Mukhopadhyay, V., Sobieszczanski-Sobieski, J., Kosaka, I., Quinn, G.,** and **Charpentier, C.** Analysis design and optimization of non-cylindrical fuselage for blended-wing-body (BWB) vehicle. AIAA paper 2002–5664, 2002.
12 **Liebeck, R. H.** Design of the blended-wing-body subsonic transport. *J. Aircr.*, 2004, **41**, 10–25.
13 **Qin, N., Vavalle, A., Le Moigne, A., Laban, M., Hackett, K.,** and **Weinerfelt, P.** Aerodynamic considerations of blended wing body aircraft. *Prog. Aerosp. Sci.*, 2004, **40**, 331–343.
14 **Kresse, N.** *VELA – very efficient large aircraft*, 2006 (Aerodays, Vienna, Austria).
15 **Scholz, D.** The blended wing body (BWB) aircraft configuration. In Proceedings of the DGLR-VDI-RAeS-HAW Praxis Seminar Luftfahrt, Hamburg, Germany, September 2006.
16 **Torenbeek, E.** Blended-wing-body and all wing airliners. In Proceedings of the 8th European Workshop on *Aircraft design education*, Samara, Russia, May–June 2007.
17 **Siouris, S.** and **Qin, N.** Study of the effects of wing sweep on the aerodynamic performance of a blended wing body. *Proc. IMechE, Part G: J. Aerospace Engineering*, 2007, **221**, 47–55. DOI: 10.1243/09544100JAERO93.
18 **Martinez-Val, R.** and **Schoep, E.** Flying wing versus conventional transport airplane: the 300 seat case. In Proceedings of the 22nd ICAS Congress, Harrogate, UK, September 2000, paper 113 (available on CD-ROM).
19 **Martinez-Val, R.** and **Perez, E.** Medium size flying wings. In *Innovative configurations and advanced concepts for future civil aircraft* (Eds E. Torenbeek and H. Deconinck), 2005, Lecture Series 2005–06, paper no. 8 (Von Karman Institute for Fluid Dynamics, Brussels, Belgium).
20 **Martinez-Val, R., Perez, E., Alfaro, P.,** and **Perez, E.** Conceptual design of a medium size flying wing. *Proc. IMechE, Part G: J. Aerospace Engineering*, 2007, **221**, 57–66. DOI: 10.1243/09544100JAERO90.
21 **Ghigliazza, H. H., Martinez-Val, R., Perez, E.,** and **Smrcek, L.** Wake of transport flying wings. *J. Aircr.*, 2007, **44**, 558–562.
22 **Martinez-Val, R., Cuerno, C., Perez, E.,** and **Ghigliazza, H. H.** Potential effects of blended-wing-bodies on the air transportation system. *J. Aircr.*, 2010, **47** (in press).
23 Annex 14. Aerodromes – aerodrome design and operation, heliports, 2003 (International Civil Aviation Organisation, Montreal, Canada).
24 **Durso, S.** and **Martinez-Val, R.** Flight dynamics of the flying wing. In Proceedings of the 26th ICAS Congress, Anchorage, Alaska, USA, paper 184, September 2008 (available on CD-ROM).
25 **Howe, D.** *Aircraft conceptual design synthesis*, 2000 (Professional Engineering Publishing, London, UK).
26 **Martinez-Val, R.** and **Perez, E.** Optimum cruise lift coefficient in initial design of jet aircraft. *J. Aircr.*, 1992, **29**, 712–714.

27 Approximate methods for estimation of cruise range and endurance: aeroplanes with turbo-jet and turbo-fan engines, ESDU 73019, 1982.

28 **Torenbeek, E.** *Synthesis of subsonic airplane design*, 1982 (Delft University Press, Delft, The Netherlands).

29 **Roskam, J.** Component weight estimation. In *Airplane design*, vol. 5, 1985 (Roskam Aviation, Ottawa, Kansas).

30 A330 airplane characteristics for airport planning, Airbus, Blagnac, France, 2005.

31 B777 airplane characteristics for airport planning, Boeing, Seattle, Washington, USA, 2008.

32 **Raymer, D. P.** *Aircraft design: a conceptual approach*, 3rd edition, 1999 (AIAA, Washington, District of Columbia).

33 **Roskam, J.** *Preliminary sizing of airplanes, airplane design*, vol. 1, 1985 (Roskam Aviation, Ottawa, Kansas).

34 **Roskam, J.** Preliminary calculation of aerodynamic, thrust and power characteristics. In *Airplane design*, vol. 6, 1987 (Roskam Aviation, Ottawa, Kansas).

35 **Scholz, D.** DOCSYS – a method to evaluate aircraft systems. Bewertung von Flugzeugen, Workshop DGLR Fachausschuss S2, Luftfahrtsysteme, Munich, 26/27 October 1998.

36 **Vasigh, B., Fleming, K.,** and **Tacker, T.** *Introduction to air transport economics*, 2008 (Ashgate, Aldershot, UK).

37 **Roskam, J.** Airplane cost estimation: design, development, manufacturing and operating. In *Airplane design*, vol. 8, 1990 (Roskam Aviation, Ottawa, Kansas).

APPENDIX

Notation

a_{tp}	speed of sound at or above the tropopause
A	wing aspect ratio
AE	specific range (Fig. 7)
c_f	friction coefficient
c_j	specific fuel consumption
c_{min}	minimum chord for habitability
C_{fuel}	fuel contribution to direct operating cost
C_{price}	contribution of price-dependent terms to direct operating cost
C_{D0}	non-lift-dependent drag term (equation (15))
C_L	lift coefficient
D	drag
DOC	direct operating cost
K	range parameter (see equations (10) to (13))
L	lift
M	Mach number
MPL	maximum payload
MTOW	maximum take-off weight
N_{pax}	number of passengers
OEW	operating empty weight
p	pressure at cruise altitude
PL	payload
R	range
Re	Reynolds number
RF	reserve fuel
S	wing area
S_{cab}	cabin area
t/c	airfoil relative thickness
TF	trip fuel
V	cruise speed
W	weight
W_f	final cruise weight
W_i	initial cruise weight
W_{to}	maximum take-off weight
Wn	abbreviation to W_{to}/N_{pax} (see equation (25))

β	parameter in equation (4)
γ	specific heats ratio (1.4)
λ	wing taper ratio
Λ	quarter chord swept angle
φ	parameter in equation (4)

Subscripts

cr	cruise
nom	nominal or design value
ref	reference from previous study [**20**]